

EXPERIMENTAL MULTI-WAVELENGTH IMAGING PYROMETER FOR REMOTE SENSING OF TEMPERATURE PROFILES ON SURFACES WITH UNKNOWN EMISSIVITY

Michael B. Kaplinsky, Jun Li, Nathaniel J. McCaffrey, Edwin S. H. Hou and Walter F. Kosonocky

Electronic Imaging Center

New Jersey Institute of Technology, Newark, New Jersey 07102-1982, USA

KEY WORDS: Radiometric Temperature Measurement, Multispectral Radiometry, Infrared Sensor

ABSTRACT

Experimental Multi-wavelength Imaging Pyrometer (M-WIP) is presented for remote sensing of temperature profiles of targets with unknown spectrally varying emissivity. A software package was developed for calibration and real-time M-WIP measurements. An experimental 7-filter line-sensing M-WIP system was implemented with a 320x122-element PtSi IR-CCD imager and an assembly of narrow-band striped IR filters in the spectral range from 1797nm through 4512nm. The M-WIP system was calibrated against a commercial blackbody source over temperature range from 450°C to 950°C. The signal processing included background subtraction, compensation for variation of dark current with detected signal and correction for non-linearities of IR imager response. Initial M-WIP measurements demonstrated real-time temperature resolution ΔT of $\pm 1^\circ\text{C}$ for blackbody target over temperature range from 600°C to 900°C. Temperature resolution of $\pm 4^\circ\text{C}$ was demonstrated for the blackbody source viewed through the double polished silicon wafer with unknown spectral transmissivity in the temperature range from 500°C to 950°C.

INTRODUCTION

The non-contact radiometric temperature measurements are based on the detection and analysis of thermal radiation emitted by an object. The underlying idea of all radiometric techniques is based on the concept of the blackbody radiator which is defined as an ideal surface that emits more thermal radiation than any other surface at the same temperature. The emission of real objects can be described by the surface emissivity, ϵ , which is defined as the ratio of radiation emitted by the real surface to that emitted by the blackbody at the same temperature.

In general, in order to infer the temperature of the target from the measurement of emitted radiation, the value of the surface emissivity, ϵ , should be known. Therefore, in the situations where the emissivity of the target is changing rapidly, or the conditions of the process preclude the independent measurements of target emissivity, the conventional radiometric methods will not yield the true temperature.

This paper presents the progress in the development of a multi-wavelength imaging pyrometer (M-WIP) for remote sensing of temperature profiles of hot surfaces with unknown wavelength-dependent emissivity. For remote temperature sensing by M-WIP, the spectral radiance of the target is measured at several distinct wavelengths by an IR-CCD camera with an assembly of 7 narrow-band filters positioned in front of its FPA. Based on these measurements the temperature and model parameters of the target emissivity are determined simultaneously from the least-squares fit of the theoretical model of IR camera output signal to the experimental data [1-4, 11].

In order to obtain high accuracy of M-WIP temperature measurements it is essential to compensate for the inherent non-linearities of the IR imager response. The signal conditioning presented in this paper includes compensation for the loss of sensor responsivity with accumulated signal level (saturation), background subtraction, and correction for the accumulated dark current charge.

This paper also presents the least-squares based algorithm for calibration of M-WIP system against reference blackbody source. This calibration utilizes wide range of blackbody temperatures and yields effective spectral and transmission characteristics of the system.

MULTI-WAVELENGTH IMAGING PYROMETER

In its most general form, the least-squares minimization problem of M-WIP can be expressed as:

$$\min_{T, \epsilon} \sum_{i=1}^N \left\{ \frac{1}{\sigma_i^2} \left[S_i - \tilde{S}(T, \epsilon, \lambda_i) \right]^2 \right\} \rightarrow T, \epsilon(\lambda) \quad (1)$$

where:

S_i - detected signal at λ_i (electrons / pixel),

$\tilde{S}(T, \epsilon, \lambda)$ - theoretical signal at λ (electrons / pixel),

T - unknown temperature of the target (K),

$\epsilon = \epsilon(\lambda)$ - emissivity model,

$\sigma_i = \Delta S_i = \sqrt{S_i}$ - rms signal noise (rms electrons/pixel)

It might be noted that in the case of M-WIP, Eq. (1) calls for minimization of the weighted sum of squares of differences between the theoretical and experimental values of the detected signal, where the points with higher values of the rms shot noise are given less weight.

Used in Eq. (1) radiometric model for the output signal of the IR imager was developed based on the reference wavelength [7] approach and is given by [2]:

$$S(\lambda, T) = K(\lambda, T) \cdot \epsilon(\lambda) \cdot R(\lambda) \cdot L_{\lambda, b}(\lambda, T) \quad (2)$$

where $L_{\lambda, b}(\lambda, T)$ is the blackbody spectral radiance, $R(\lambda)$ is the spectral responsivity of the imager, and $K(\lambda, T)$ is the correction coefficient, which depends on the effective transmission of the camera optical system, $\tau(\lambda)$, the geometry of the detector and the optical integration time.

It can be shown that the accuracy of the least squares based M-WIP temperature measurement strongly depends on the selected emissivity model [2]. In order to correctly determine the temperature of the target with unknown emissivity, it is necessary to provide a sufficiently complex and flexible emissivity model that is capable of accurately approximating the target spectral emissivity. On the other hand, a too complex, overdetermined model, will lead to a decrease in the resulting temperature accuracy of the measurement due to the redundant degrees of freedom which it introduces in the fitting algorithm. Analysis of the published data on the spectral emissivity of various materials [8] shows that in most cases the spectral emissivity can be adequately represented by a polynomial function of wavelength:

$$\epsilon(\lambda) = a_0 + a_1 \cdot \lambda + a_2 \cdot \lambda^2 + \dots \quad (3)$$

where a_0, a_1, a_2 are the parameters of the emissivity model.

However, our theoretical and experimental studies [9] of the spectral emissivity of silicon using Fourier Transform Infrared (FTIR) Spectroscopy (that may also apply to other semiconductor and metallic surfaces) indicate that the emissivity is most accurately approximated by polynomial functions of wavenumber as:

$$\epsilon(\lambda) = a_0 + \frac{a'_1}{\lambda} + \frac{a'_2}{\lambda^2} + \dots \quad (4)$$

EXPERIMENTAL M-WIP SYSTEM

As illustrated by the schematic diagram in Fig. 1, the experimental M-WIP system consists of an IR camera with associated electronics, an IR filter assembly, and an image data processing system.

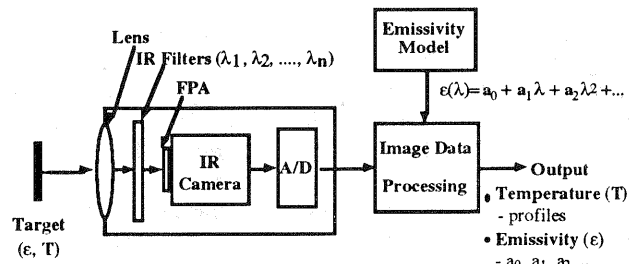


Fig. 1. Multi-wavelength imaging pyrometer (M-WIP)

IR Camera

The experimental multi-wavelength imaging pyrometer uses a Samoff 320x244 PtSi IR-CCD camera [5]. For the purpose of radiometric imaging, the camera is operated in a non-interlaced mode with 320x122 pixels and automatically selectable optical integration times in the range from 120μs to 12s or longer [4,10]. The operation of the camera with variable optical integration time increases its effective dynamic range and allows to accommodate a wide range of optical signal levels. Subframe integration time control was achieved by employing a double detector readout. To facilitate this operation, camera circuitry was developed for automatically controlling the CCD waveforms to operate at the required integration time. This imager was also operated in a multi-frame integration mode with a single detector readout for optical integration times in multiples of 33ms. The analog video signal was digitized to 12-bits resolution. Circuits were also developed to embed critical information in the video signal to facilitate radiometric post-processing. An optoelectronically buffered digital interface was developed to connect the camera system to a DATACUBE image processing system.

M-WIP Filters

The experimental M-WIP presented here is based on a line-sensing filter assembly with 7 narrow-band filters mounted on FPA packaging. The line-sensing assembly uses f/1.4 spherical lens in order to focus the image of the radiant target on the narrow horizontal slit. The image of the target area defined by the slit aperture is then refocused on FPA in horizontal direction using cylindrical lens as illustrated in Fig. 2. As a result the image of the horizontal line on the target surface is "spread" across all M-WIP filters in vertical direction while preserving horizontal resolution.

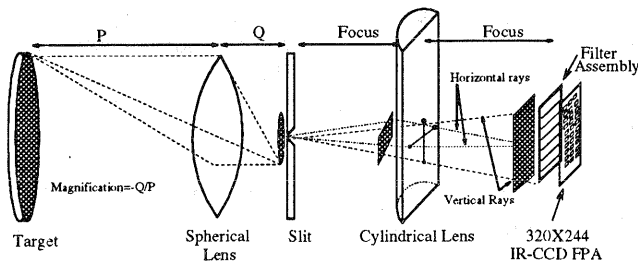


Fig. 2. Filter optics for M-WIP (shaded areas represent optical images)

The central wavelengths, λ_0 , of M-WIP filters ranging from 1797nm to 4512nm (at cryogenic temperature of 77K) correspond to the spectral sensitivity of the PtSi Schottky-barrier detectors (SBDs) used in the camera. The bandwidths of the filters at half of peak transmission range from 47 nm for the 1797-nm filter to 102 nm for the 4512-nm filter. The values of the peaks of the filter transmissions were individually attenuated in order to provide approximately equal detected signal at all wavelengths for blackbody target at 700°C. The attenuation of the IR filters in this manner partially compensates for the spectral variations in the detected signal levels and, therefore, reduces the requirements on the dynamic range of the camera.

Image Data Processing System

Image data processing for M-WIP is based on the DATACUBE MaxVideo system using a SUN workstation as the host computer. The DATACUBE MaxVideo system is a user configurable real-time image acquisition and processing system. It consists of a number of modules that can be interconnected to suit the image processing task. The modules are housed in a 20 slot VME chassis box (MAX-BOX) while a SUN 4/330 acts as the host computer. The system can operate at a maximum data rate of 10 MHz. In our system, we have one MAX-SCAN data acquisition module, two ROI-STORE 512Kbytes memory modules, three MAX-SP general purpose signal processing modules and one MAX-GRAPH video and graphics display module. A custom developed display board is used to reformat the 320x122 image for standard RS-170 display. The development software for the MaxVideo system is ImageFlow which consists of a set of C-callable libraries.

EXPERIMENTAL RESULTS

Compensation for Inherent System Non-Linearities

In order to obtain high radiometric accuracy of the M-WIP measurements, we have found it necessary to compensate for non-linearities of the IR imager response [3,4]. In the case of the PtSi IR-CCD imager used in the experimental M-WIP system, both the dark current and the spectral responsivity of the Schottky-barrier detectors (SBDs) depend on the SBD bias voltage and decrease with increasing level of integrated charge signal. This dependence of the dark current and responsivity on the detected signal is especially pronounced at high signal levels resulting in a "saturation-type" non-linearity. On the other hand, the reduction of the signal due to apparent charge trapping losses is especially evident at low signal levels and represents "offset-type" non-linearity.

In order to correct the detected signal for the dark current charge, the suppression of the dark current due to high signal level can be estimated according to the following algorithm:

1. Using cold-shield to prevent radiative flux from reaching the detectors, the dark current charge is experimentally measured for a wide range of optical integration times [3,4]. The dark current is then approximated by an exponential function of integration time, t_{int} , as:

$$S_{DC}^{measured} = ae^{bt_{int}} + c \quad (5)$$

A derivative of Eq. (5) with respect to optical integration time, t_{int} , represents the dark current which can be expressed as function of the accumulated signal:

$$I_{DC}(S_{DC}^{measured}) = I_{DC}(S) = \frac{\partial S_{DC}^{measured}}{\partial t_{int}} = b(S_{DC}^{measured} - c) = b(S - c) \quad (6)$$

where S represents the total accumulated charge regardless of its source.

2. The dark current component of the signal integrated by the imager viewing the radiant target can now be expressed as:

$$S_{DC}^{estimated}(T, t_{int}) = \int_0^{t_{int}} I_{DC}(S(T, t_{int})) dt = \frac{b}{k_2} (S(T, t_{int}) - k_1 - k_3) + b(k_3 - c)t_{int} \quad (7)$$

where $S(T, t_{int}) = k_1 e^{k_2 t_{int}} + k_3$ is the detected signal approximated by the exponential function of optical integration time, t_{int} , and T is the temperature of the radiant target.

Figure 3 illustrates the experimentally measured dark current charge, $S_{DC}^{measured}$, and the estimated dark current charge, $S_{DC}^{estimated}$, corresponding to the imager viewing the blackbody target at 500°C, 600°C, 700°C, and 800°C through the 4512-nm filter.

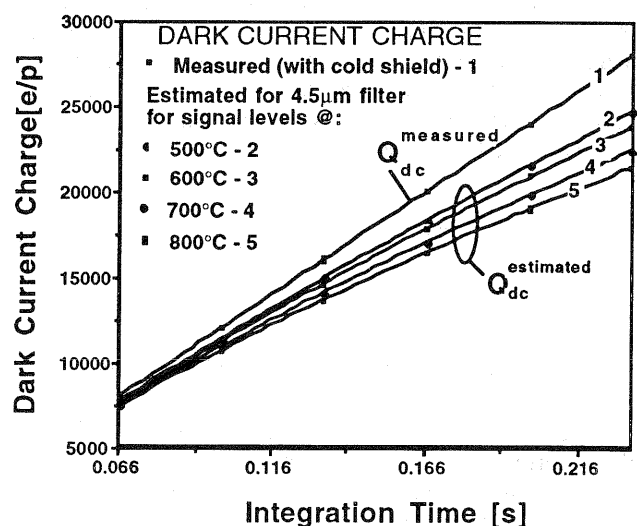


Fig. 3. Measured and estimated dark current

In order to compensate for saturation non-linearity of the imager response it was assumed that this non-linearity represents the loss of the detector responsivity with rising bias voltage and, therefore, it is primarily a function of the detected signal level.

The pixel-by-pixel correction for offset and saturation non-linearities of IR imager response is achieved according to the following algorithm:

1. Based on the experimental signal measurements for a wide range of blackbody temperatures and values of the optical integration time, the detected signal can be approximated by an exponential function of optical integration time, t_{int} , for each temperature, T_i , of the calibration source, as:

$$S^{detected} = a_1^i e^{a_2^i t_{int}} + a_3^i \quad (8)$$

2. For N various radiative fluxes corresponding to N various temperatures, T_i , of the calibration blackbody source the intensity of the incident on IR detectors radiative flux is characterized by the ratio of the detected signal, $S(T_i, t_{int})$, to the value of optical integration time, t_{int} , as:

$$F_i = \frac{S(T_i, t_{int})}{t_{int}}, i = 1, \dots, N \quad (9)$$

3. The linearized signal corrected for off-set at zero integration time can now be expressed as function of the detected signal and the intensity of the incident radiative flux as:

$$S^{linear} = \left. \frac{\partial S^{detected}}{\partial t_{int}} \right|_0 \times t_{int} = a_1^k \cdot a_2^k \cdot t_{int} = a_1^k \cdot \ln \left(\frac{S^{detected} - a_3^k}{a_1^k} \right) \quad (10)$$

where index k is determined from the following condition (assuming that F_k are sorted in the ascending order):

$$\frac{F_k + F_{k-1}}{2} < \frac{S^{detected}}{t_{int}} < \frac{F_k + F_{k+1}}{2} \quad (11)$$

The radiative flux intensities used for M-WIP calibration, F_i , are stored in the ascending order along with corresponding coefficients a_1^i and a_3^i in the correction table for each pixel. During the on-line M-WIP temperature measurements these tables are searched according to the criteria given by Eq. (11). Once the appropriate flux level, F_k , has been determined, the corresponding correction coefficients a_1^k and a_3^k are then used for signal linearization according to Eq. (10).

Figure 4. illustrates the correction for saturation non-linearity resulting from application of the above algorithm to the signals detected by M-WIP through 4500nm filter illuminated by the blackbody source at 600°C.

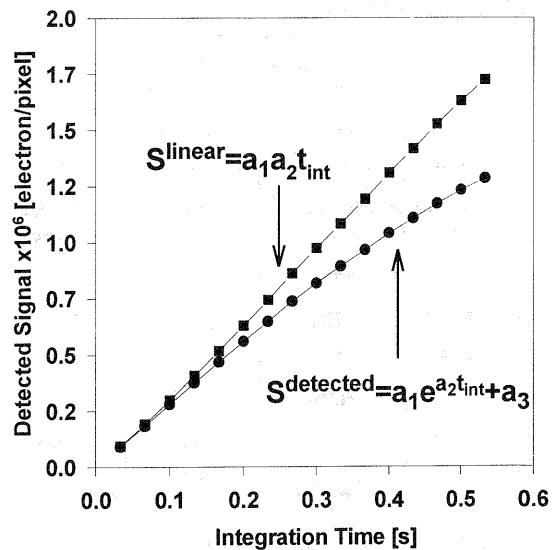


Fig. 4. Saturation non-linearity correction.

Calibration of M-WIP System

The experimental M-WIP system includes a least-squares-based calibration algorithm [1-3] for evaluation of effective values of peak filter transmissions (τ_o) and center wavelengths (λ_o) based on the detection of radiation emitted by the pre-calibrated blackbody source over a wide range of temperatures:

$$\min_{\tau_o, \lambda_o} \sum_{i=1}^M \left\{ \frac{1}{\sigma_i^2} \left[S_i - \tilde{S}(T_i^{BB}, \tau_o, \lambda_o) \right]^2 \right\} \rightarrow \tau_o, \lambda_o \quad (12)$$

where:

T_i^{BB} - i -th temperature of reference blackbody source,

$\sigma_i = \Delta S_i = \sqrt{S_i}$ - rms signal noise (rms electrons/pixel)

A seven-filter experimental M-WIP system was initially calibrated according to Eq. (12) against a reference blackbody source over a temperature range from 450°C to 900°C. It should be noted that the initial calibration did not include the compensation for saturation non-linearity of the imager response. This calibration resulted in an effective radiometric uniformity correction of all camera pixels used for the M-WIP measurements. However, due to self-compensation for non-linear response of the imager by the calibration algorithm, the initial calibration resulted in a shift of the effective center wavelengths of the filters in the range of 28 to 358 nm as compared to manufacturer specifications (see column II of Table 1). In order to study this effect, the M-WIP "calibration" was also performed on the basis of the simulated signal with various values of "offset" and "saturation" non-linearities. It was found, as illustrated in column III of Table 1, that "offset" non-linearity of 2.5% of Q_{max} at zero optical integration time (i.e. $t_{int}=0$) and "saturation" non-linearity of 8% at 50% of Q_{max} results in similar shifts in effective center wavelengths of IR filters as was obtained for the experimental data not compensated for imager non-linearity.

Table 1. Calibration of M-WIP filters

No	$\Delta\lambda$ (nm)	Center Wavelength, λ_0 (nm)			
		I OFC Specs	II Initial M-WIP Calibration	III M-WIP Estimated	IV Final M-WIP Calibration
1	51	1790	2004	2007	1758
2	64	2180	2220	2258	2174
3	60	2580	2721	2792	2446
4	38	3158	3186	3227	2961
5	60	3447	3696	3645	3113
6	77	3970	4175	4267	3756
7	102	4536	4870	4846	4594

Poor quality of the initial calibration led to the incorporation of the correction for "saturation-type" response non-linearity into the final version of the signal conditioning algorithm. As shown in the column IV of Table 1, the correction for "saturation" non-linearity of imager response resulted in the calibration of M-WIP filters with the center wavelengths representing a much closer match to the manufacturer's specifications.

Demonstrated temperature resolution of M-WIP

The quality of the least-squares fit of the theoretical M-WIP signal model to the experimentally detected signal corresponding to blackbody target at various temperatures is illustrated in Fig. 5. It should be noted that the presented results were normalized to the transmission characteristics of filter No. 1.

Using the M-WIP calibration with the correction for "saturation" non-linearity, we have achieved an accuracy of $\pm 1.0^\circ\text{C}$ for real-time temperature measurements of the center of the blackbody aperture in the range from 650°C to 900°C as illustrated in Fig. 6.

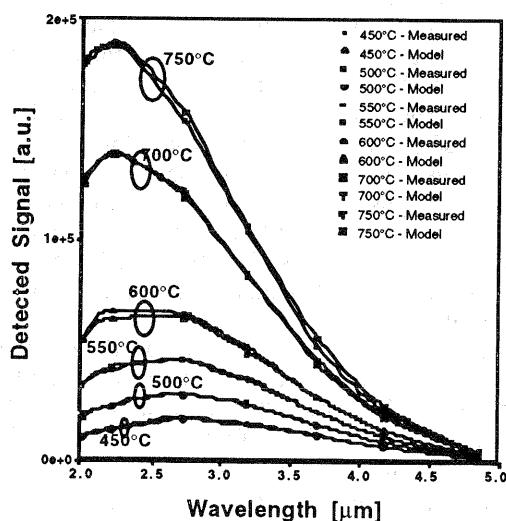


Fig. 5. Measured and M-WIP modeled signal levels for blackbody target temperatures from 450 to 750°C

In order to study the accuracy of M-WIP temperature measurements for targets with spectrally varying emissivity, a double-polished silicon wafer was placed in the optical path of M-WIP system. The blackbody source was then imaged onto M-WIP filter assembly through a silicon wafer acting as a broadband filter with spectrally varying transmission. In this set-up the spectral characteristics of the radiation incident on the M-WIP imager are given by the product of the blackbody radiation (given by the Planck's equation) and spectral transmission of the double-polished silicon wafer. Therefore, for this test the radiation incident on the M-WIP imager corresponds to that of radiant target with temperature equal to the temperature of the blackbody source and the spectral emissivity of the double-polished silicon wafer.

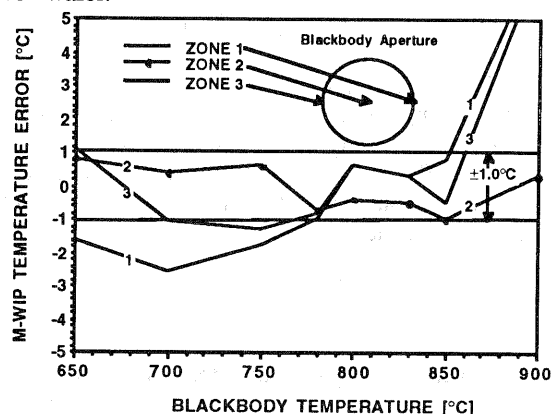


Fig. 6. Real-time M-WIP measurements of blackbody temperature after implementation of on-line correction for "saturation" non-linearity.

As shown in Fig. 7, based on the optical arrangement described above we have demonstrated the accuracy of $\pm 4^\circ\text{C}$ for off-line temperature measurements of the location corresponding to the center of silicon wafer in the temperature range from 500°C to 950°C . The corresponding M-WIP estimate of the spectral transmissivity of double-polished silicon wafer is:

$$\tau(\lambda) = 0.4893 + 0.017 \cdot \lambda \quad (13)$$

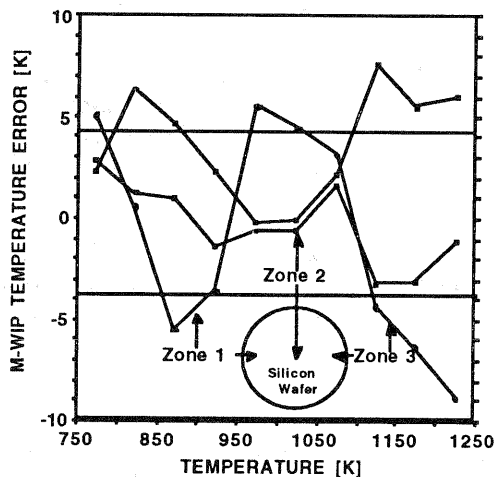


Fig. 7. M-WIP measurements of target temperature with effective emissivity equal to the transmissivity of double-polished silicon wafer.

CONCLUSIONS

- A multi-wavelength imaging pyrometer (M-WIP) was presented for remote sensing of temperature profiles of gray and color targets with unknown emissivities and software package was developed for calibration and real-time M-WIP measurements. An experimental 7-filter line-sensing M-WIP system was implemented with a 320x122-element non-interlaced PtSi IR-CCD radiometric camera capable of operation with optical integration times ranging from 0.12ms to 12 s, thus providing wide dynamic range.
- After calibration against a commercial blackbody reference source in the temperature range from 500°C to 950°C, temperature resolution of $\pm 1^\circ\text{C}$ was demonstrated with the experimental M-WIP system for real-time temperature measurement of the blackbody source in the temperature range from 600°C to 900°C.
- The study of the accuracy of M-WIP temperature measurements for targets with spectrally varying emissivity was conducted using double-polished silicon wafer placed in the optical path of M-WIP system. Temperature resolution of $\pm 4^\circ\text{C}$ was demonstrated with the experimental M-WIP system for blackbody source viewed through the double polished silicon wafer with unknown spectral transmissivity in the temperature range from 500°C to 950°C.
- To achieve the above performance, the radiometric IR-CCD camera was operated with black level and background subtraction, a compensation for dark current charge corresponding to radiant target and background signal levels (including correction for the variation of SBD dark current with signal level), and correction for saturation non-linearity of the imager response as function of the accumulated signal and the intensity of the incident radiative flux.

ACKNOWLEDGMENTS

This work was supported by the US Air Force Wright Laboratory and the ARPA Microelectronics Technology Office under Contract No. F33615-92-C-5817.

REFERENCES

1. M.B. Kaplinsky, W.F. Kosonocky, N.J. McCaffrey, J. Li, E.S. Hou, C.N. Manikopoulos and N.M. Ravindra, "Multi-Wavelength Imaging Pyrometer for Non-Contact Temperature Sensing," Proceedings of IEEE International Symposium on Industrial Electronics, Athens, Greece (July 1995)
2. M.B. Kaplinsky, "Application of Imaging Pyrometry for Remote Temperature Measurement," Masters Thesis, New Jersey Institute of Technology (1993)
3. W.F. Kosonocky, M.B. Kaplinsky, N.J. McCaffrey, E.S. Hou, C.N. Manikopoulos, N.M. Ravindra, S. Belikov, J. Li and V. Patel, "Multi-Wavelength Imaging Pyrometer," SPIE Proceedings, Vol. 2225-04, Orlando, FL (1994)
4. N.J. McCaffrey, M. Kaplinsky, B. Esposito, and W.F. Kosonocky, "Radiometric Performance of 640x480 and 320x244 PtSi IR Cameras," SPIE Proceedings, Vol. 2225-05, Orlando, FL (1994)
5. T.S. Villani, W.F. Kosonocky, F.V. Shallcross, J.V. Groppe, G.M. Meray, J.J. O'Neill III, B.J. Esposito, "Construction and Performance of a 320X244-Element IR-CCD Imager with PtSi SBDs," SPIE Proceedings, Vol. 1107-01 (1989)
6. W.F. Kosonocky, "State-of-the-Art in Schottky-Barrier IR Image Sensors," SPIE Proceedings, Vol. 1685-2, Orlando, FL (1992)
7. P.B. Coates, "Wavelength Specification in Optical and Photoelectric Pyrometry," Metrologia, 13, 1 (1977)
8. D.P. DeWitt and J.C. Richmond, "Thermal Radiative Properties of Materials," in Theory and Practice of Radiation Thermometry, John Wiley & Sons, New York (1988)
9. N.M. Ravindra, et. al., "Development of Emissivity Models and Induced Transmission Filters for Multi-Wavelength Imaging Pyrometry," SPIE Proceedings, Vol. 2245-48, Orlando, FL (1994)
10. N.J. McCaffrey, "Design of a 320X122 MWIR-CCD PtSi Imaging Radiometer with Automatic Optical Integration Time Control," Masters Thesis, New Jersey Institute of Technology (1993)
11. M.A. Khan, et. al., "Noncontact Temperature Measurement: Least Squares Based Techniques," Rev. Sci. Instrum. 62, 403 (1991)
12. W.H. Press, S.A. Teukolsky, W.T. Vetterling and B.P. Flannery, "Numerical Recipes in C: the art of scientific computing," Cambridge University Press (1992)